

INTEGRITY ASSESSMENT OF BURIED PIPE IN EROSION ENVIRONMENT

ZULKIFLI BIN ABDUL MAJID

A thesis submitted in fulfilment of the
requirements for the award of the degree of
Doctor of Philosophy (Gas Engineering)

Faculty of Chemical and Energy Engineering
Universiti Teknologi Malaysia

SEPTEMBER 2017

Specially dedicated to my beloved late mother and father,
wife, my dear sons and daughters
those who had taught me useful lessons, provided continuous guide
and relentless love and support to me in my life.

ACKNOWLEDGEMENT

I wish to express my sincere appreciation and gratitude to my supervisor, Professor Dr. Rahmat Mohsin for his continuous encouragement, guidance, moral supports, and laborious discussions throughout the period of studies. Professor Dr. Mohd. Zamri Yusoff is also highly acknowledged for his comments and suggestion in this research work. I am deeply inspired and motivated by their commitments.

I am also dedicating my special thanks to Mr. Jamal Asri Othman, Mr. Abu Samah Nasir, Mr. Mohd. Redhuan Ramlee, Mr. Mohd. Zaid Rozlan, Mr Ahmad Osman, Ms. Siti Fairuz Juiani, Mr. Fadli Omar and Mr. Mohd. Firdaus for their critical comments, ideas and kind efforts in providing their helping hands and facilitates the overall research project. Without their continuous support and interest, this project would not have been a success.

My sincere appreciation also extends to my close friends from Universiti Malaysia Pahang, Professor Dr. Zulkefli Yaacob and Professor Zulkafli Hassan and friends who have assisted and supported me throughout my research tenure with their knowledge and friendship. Their views and tips are useful indeed.

ABSTRACT

The integrity assessment of API 5L X42 carbon steel pipe in terms of erosion effect due to impaction of high pressure erosive slurry was studied. A water jet structure was analysed using a transparent perspex water filled tank. This was followed by buried pipe erosion study in a sieved sand as a backfilling material in a specially designed submerged experimental rig. Computational fluid dynamics (CFD) technique was applied to simulate numerically the pipeline erosion characteristics in comparison to the experimental findings. The sieved results indicated that majority of the backfilling materials; made up by quartz mineral having a size of 0.2 to 2.0 mm, was in angular shape. The impaction of sand-water slurry on the pipe wall produced two peculiar regions; smooth surface in the middle and surrounded by rough wavy surface. The smooth surface was formed due to the high-pressure water jet (potential core) perpendicular to the centre of the pipe surface. On contrary, the rough surface was formed due to the impact of sand-water in cutting action mode at the upper and bottom part of the pipe, as the water stream was being deflected radially. In comparison, the bottom part of the pipe experienced higher thickness reduction than the upper area. The average thickness reduction of the pipe wall due to the impaction of orifice jetting was 5.68% higher than that of the nozzle jet. The locations of ring type contours of water and sand wall shear from CFD simulation were found to be similar as the experimental findings. The contours of sand and water wall shear were found to be 68.67 kPa and 0.1054 kPa, respectively, at the upper and bottom sections of the pipe wall that corresponded to the higher thinning rate areas as in the experimental study. At the point of impaction that was perpendicular to the pipe surface, the sand and water wall shear stresses were found to be 13.73 kPa and 0.2208 kPa, respectively, this concurred by the smooth convex region on the pipe surface from the experimental results. Percentage of wall thinning rate from the experimental study (10.74%) was found to be comparable to CFD simulation results with the percentage difference of sand and water were 11.12% and 11.02%, respectively. It is therefore concluded that at 400 mm separation distance, the pipeline was found to be safe from any erosion effect of 1000 kPa water jetting, this could be considered for gas industry application.

ABSTRAK

Penaksiran integriti paip keluli karbon API 5L X42 dari aspek kesan hakisan akibat hentaman buburan hakis bertekanan tinggi telah dikaji. Struktur jet air telah dianalisis menggunakan tangki perspeks lutsinar yang dipenuhi air. Ini diikuti dengan kajian hakisan paip tertimbus dalam pasir bertapis sebagai bahan kambusan dalam rig uji kaji terbenam yang direka khas. Teknik dinamik aliran pengiraan (CFD) telah digunakan untuk mensimulasi secara berangka sifat hakisan talian paip berbanding dengan hasil uji kaji. Keputusan tapisan menunjukkan majoriti bahan kambusan tersebut; yang terdiri daripada mineral kuartza yang bersaiz antara 0.2 hingga 2.0 mm, adalah rupa bentuk bersegi. Hentaman buburan pasir-air terhadap dinding paip menghasilkan dua rantau yang khusus iaitu; permukaan licin di bahagian tengah dan permukaan kasar beralun di sekeliling. Permukaan licin dihasilkan oleh jet air bertekanan tinggi (potensi teras) yang bersudut tepat di bahagian tengah permukaan paip. Permukaan kasar pula dibentuk oleh hentaman pasir-air secara mod tindakan memotong di bahagian atas dan bawah paip apabila arus air dipesongkan secara kejejaran. Jika dibandingkan, bahagian bawah permukaan paip mengalami pengurangan ketebalan paip yang lebih tinggi daripada bahagian atas. Purata pengurangan ketebalan dinding paip disebabkan oleh jet orifis adalah 5.68% lebih tinggi berbanding jet muncung. Lokasi kontur jenis gelang bagi dinding ricih air dan pasir daripada hasil simulasi CFD didapati adalah serupa dengan keputusan eksperimen. Kontur bagi dinding ricih pasir dan air adalah masing-masing 68.76 kPa dan 0.1054 kPa di bahagian atas dan bawah dinding paip yang mana bertepatan dengan kawasan yang mengalami kadar pengurangan ketebalan yang lebih tinggi dalam eksperimen. Pada titik hentaman yang bersudut tepat dengan permukaan paip, tegasan ricih dinding pasir dan air adalah masing-masing 13.73 kPa and 0.2208 kPa, dan ini disokong oleh kawasan cembung yang licin pada permukaan paip oleh keputusan eksperimen. Peratus kadar penipisan dinding daripada eksperimen (10.74%) didapati setanding dengan keputusan simulasi CFD yang mana peratus perbezaan pasir dan air adalah masing-masing 11.12% dan 11.02%. Adalah disimpulkan bahawa pada kedudukan 400 mm jarak pemisahan, talian paip didapati selamat daripada sebarang kesan hakisan akibat hentaman jet air bertekanan 1000 kPa dan sesuai dipertimbangkan bagi aplikasi industri gas.

TABLE OF CONTENTS

CHAPTER	TITLE	PAGE
	DECLARATION	ii
	DEDICATION	iii
	ACKNOWLEDGEMENT	iv
	ABSTRACT	v
	ABSTRAK	vi
	TABLE OF CONTENTS	vii
	LIST OF TABLES	xii
	LIST OF FIGURES	xiv
	LIST OF ABBREVIATIONS	xix
	LIST OF SYMBOLS	xxi
	LIST OF APPENDICES	xxviii
1	INTRODUCTION	1
	1.1 Background and Motivation	1
	1.2 Problem Statement	5
	1.3 Research Hypothesis	8
	1.4 Objectives	8
	1.5 Scope of Study	9
	1.6 Limitation of Study	9
	1.7 Significance of Study	10
	1.8 Thesis Organization	11

2	LITERATURE REVIEW	13
2.1	Introduction	13
2.2	Failure Associated with Natural Gas Transportation and Distribution	17
2.3	Theory of Jets	19
2.3.1	Structure and Development of a submerge Free Jet	20
2.3.2	Jet Instabilities and Formation of Vortices	23
2.3.3	Jet Impingement	25
2.3.3.1	Jet Impingement on Flat Surface	25
2.3.3.2	Impingement of Jets on Convex Surface	29
2.4	Erosion	32
2.4.1	Types of Erosion	33
2.4.1.1	Liquid Impact	33
2.4.1.2	Erosion-Corrosion	35
2.4.1.3	Slurry Erosion	36
2.5	Characteristic of Ductile Material	40
2.6	Factors Affecting Slurry Erosion	45
2.6.1	Particle Impact Velocities	45
2.6.2	Particle Properties	47
2.6.3	Impingement Angle	48
2.7	Design and Specification for Underground/Buried Pipeline	52
2.8	Backfilling Materials for Natural Gas Pipeline	55
2.8.1	Characteristic of Backfilling Material	55
2.8.2	Soil Analysis	57
2.8.2.1	Particle Size Distributing	58
2.8.2.2	Mineral Composition	60
2.8.2.3	Particle Shape and Angularity	61
2.9	Erosion Models	62
2.9.1	Finnie's Model	63
2.9.2	Bitter's Model	64
2.9.3	Ahlert's Model	67
2.9.4	Neilson's and Gilchrist's Model	68
2.9.5	Forder's Model	69

2.9.6	Huang's Model	71
2.10	Computation Fluid Dynamics Simulation	73
2.10.1	Governing Equation of Fluid Motion	74
2.10.2	Particle Tracking	76
2.10.3	Erosion Prediction	80
2.10.4	The Rossin-Ramler Particle Distribution Method	81
2.10.5	CFD Works Related to Erosion	82
3	METHODOLOGY	87
3.1	Introduction	87
3.2	Water Jetting Erosion Study	88
3.2.1	Water Jet Dispersion Rig	89
3.2.2	Development of Pipeline Erosion Rig	90
3.2.2.1	Pipe Sample	93
3.2.2.2	Component of Experimental Rig	94
i.	Pipe Holder Segment	94
ii.	Water Reservoir Unit	94
iii.	Experimental Tank	95
iv.	Chain Locking Lifting Mechanism	96
v.	Water Pump	97
vi.	Water Jet System	97
vii.	Water Level Indicator	98
viii.	Thickness Gauges	99
ix.	Templates for Data Taking	100
3.2.3	Experimental Procedures	101
3.2.3.1	Water Jet Dispersion	102
3.2.3.2	Pressure Measurement Procedures	103
3.2.3.3	Backfilling Soil Study	105
i.	Sampling of Backfill Material	105
ii.	Determination of Particle Size Distribution	107
iii.	Determination of Minerals Composition	108
iv.	Determination of Particle Shape	109
v.	Sieve Test on the Model Backfilling Material	109

3.2.3.4	Sand Sieve Procedure	110
3.2.3.5	Experimental Tank Preparation	111
3.2.3.6	Specimen Preparation	111
3.2.3.7	Rig immersion and Pulling Off	113
3.2.3.8	Method of Data Taking	116
3.3	Computational Simulation Study	117
3.3.1	CFD Methodology	117
3.3.3.1	Geometry	118
3.3.3.2	Computational Grid (Meshing)	119
3.3.3.3	Boundary Conditions	120
3.3.3.4	CFD Solver	122
4	RESULTS AND DISCUSSIONS	124
4.1	Introduction	124
4.2	Water Jet Dispersion	125
4.2.1	Summary of Experimental Methods	125
4.2.2	Profiling of Jets	127
4.3	Pressure and Force Profile	131
4.3.1	Summary of Experimental Methods	131
4.3.2	Pressure and Force Profile for Orifice and Nozzle Jetting	132
4.4	Erosion Morphology on Pipe Surface	139
4.4.1	Characteristics of Backfilling Material	140
4.4.1.1	Summary of Experimental Methods	140
4.4.1.2	Particle Size	140
4.4.1.3	Mineral Content	145
4.4.1.4	Particle Shape	146
4.4.1.5	Particle Size Distribution (Backfilling Material) for Erosion Study	149
4.5	Experimental Study on Erosion of Pipe Surface	155
4.5.1	Summary of Experimental Methods	155
4.5.2	Result and Discussion	155
4.6	Thinning Patterns of Pipe Wall Surface	160
4.6.1	Summary of Experimental Methods	160
4.6.2	Relationship Between Specimen Thickness and Time	160

4.6.3 Distribution of Pipe Thinning Rate	172
4.7 Comparison of Erosion Pattern Between CFD Simulation and Experimental	176
4.7.1 Effect of Jetting Size	178
4.7.2 Effect of Sand Particles Size	180
4.7.3 Effect of Sand Compactness	182
4.7.4 Effect of Separation Distance	184
4.7.5 Comparison of CFD Simulation and Experimental Results	190
4.8 Summary	192
5 CONCLUSIONS AND RECOMMENDATIONS	195
5.1 Conclusions	195
5.2 Recommendations	196
REFERENCES	198
Appendices A-G	211-239

LIST OF TABLES

TABLE NO.	TITLE	PAGE
2.1	Summary of effect of impingement angle on erosion comparison from various researcher	50
2.2	Pipeline cover requirement	54
2.3	Natural gas pipelines location classification	54
2.4	Embedded soil classes	56
2.5	Maximum particle size for different DN	56
2.6	Particle size according to ASTM D2488	57
2.7	Mohs hardness scale	60
2.8	Roundness value and particle shape	62
2.9	Erosion model empirical constant	67
2.10	Cutting and deformation velocity characteristics	71
2.11	Value of the coefficient	72
2.12	Empirical constant for turbulence model	76
2.13	Summary of the CFD study by various researchers	83
3.1	Physical parameters of pipe	93
3.2	Summary of experimental testing performed	101
3.3	Depth of sample and sample label	106
3.4	Characteristics of mineral	108
4.1	Percentage of sand in the backfill samples with size between 0.063 to 2.0 mm	141
4.2	Sand particles based on grain size	142
4.3	Composition of sand	145
4.4	Properties of mineral	146
4.5	Calculation of particles shape	148
4.6	Particle shape of backfill materials	148

4.7	Example of sieve test results (Sand model 1)	150
4.8	Particle size distribution for the model backfill materials	150
4.9	Average cumulative passing (%) for the actual and model backfill materials	151
4.10	Average thinning rate for orifice and nozzle (5 mm diameter)	173
4.11	Summary of CFD simulation study	177

LIST OF FIGURES

FIGURE NO.	TITLE	PAGE
1.1	Arrangement of failed pipes	6
1.2	Pipeline Layouts	6
2.1	Natural gas transmission system in Peninsula Malaysia	14
2.2	Natural gas distribution system in Malaysia	15
2.3	Cover Protection for buried pipelines external of building of (a) public and (b) private land area	16
2.4	Causes of natural gas transmission pipeline significant incidents	17
2.5	Significant distribution system incidents by cause	18
2.6	Free jet flow	19
2.7	Free jet structures in the axial coordinate	21
2.8	Profile of turbulence free jet	21
2.9	Free jet structures in radial coordinate	22
2.10	Formation of shear layer surround the potential core	23
2.11	Formation of vortex	24
2.12	Shear layer instabilities in a jet	25
2.13	Impingement jet zones	26
2.14	Impingement of jet on flat surface	27
2.15	Direction of flow for impinging jet	28
2.16	Vortices around the impacted wall	28
2.17	The flow of jet impingement of pipe surface	31
2.18	Flow image of jet impingement upon (a) flat-surface (b) $D/d=4$, (c) $D/d=2$ and (d) $D/d=1$. D and d is cylindrical and nozzle diameter respectively	31

2.19	The schematic illustration of material removal mechanism of liquid impact erosion	34
2.20	Mechanism of cavities erosion: (a) Mechanism of bubble Collapse and (b) Experimental evidence of damage by cavitation	34
2.21	The development of erosion corrosion pits by turbulence eddy	35
2.22	Effect of flow media (a) Low viscosity (b) High viscosity on slurry erosion	37
2.23	Flow movement of suspended particle about cylinder for low (above) and high (below) viscosity	38
2.24	Effect of flow on erosion	39
2.25	The deformation and cutting wear for ductile material	40
2.26	Surface profiles of slurry wear	43
2.27	Erosion profile with respect to (a) testing times and (b) velocities	44
2.28	Schematic diagrams showing three types of plastic deformation influenced by impingement angle of the impacted particles	49
2.29	Trench cross section (ASTM D2321)	53
2.30	Example of particle size distribution curve	58
2.31	Void spaces with respect to PSD for (a) Well-graded and (b) Poorly-graded samples	59
2.32	Particle shape and abrasiveness	61
2.33	Image of particles	62
3.1	Experimental activity flow process	89
3.2	Water jetting chamber using Perspex's model	90
3.3	Basic concepts of experimental apparatus	91
3.4	Schematic diagram of the experimental rig	92
3.5	Pipe sample arrangement	93
3.6	Pipe holder segment	94
3.7	Water reservoir unit	95
3.8	Experimental tank	96
3.9	Chain locking lifting system	96
3.10	Multistage screw-type water pump	97

3.11	Water jet nozzle	98
3.12	Water level indicator	99
3.13	Thickness gauges	99
3.14	Data taking template configurations	100
3.15	Orifice and nozzle with different port diameter	102
3.16	Cross sectional view of the orifice and nozzle	103
3.17	Pressure measurement for nozzle jetting	104
3.18	Soil Sampling	106
3.19	Location of auger hole	106
3.20	Particle sieve apparatus	107
3.21	Grains from sieve test	108
3.22	Stereo microscope for determining particle shape	109
3.23	Sand sieving process and storage tank	110
3.24	The pumping of sand-water slurry	111
3.25	Determination of points and lines	112
3.26	Pipe thickness measurements	112
3.27	Cleaning of small jetting holes	114
3.28	Rig immersion process	114
3.29	Rig pulling-off	115
3.30	Pipe wall thickness measurements	115
3.31	Location of measurement marks	116
3.32	Point of thickness measurement	116
3.33	CFD simulation methodology	118
3.34	Computational domain and boundary condition in 3D view	119
3.35	Generated mesh used in simulation process	121
4.1	Jets dispersion pattern	126
4.2	Close-up section of the jet dispersion	128
4.3	Erosion scar on surface of pipe showing ripple marks	130
4.4	Comparisons of measured and predicted pressure distribution along the jet for 3 mm diameter orifice	132
4.5	Comparisons of measured and predicted pressure distribution along the jet for 5 mm diameter orifice	133
4.6	Comparisons of measured and predicted pressure distribution along the jet for 7 mm diameter orifice	133

4.7	Pressure decay against distance for orifice with 1, 3, 5, 7, 9 and 11 mm diameters by CFD simulation.	134
4.8	Force decay against distance for orifice with 1, 3, 5, 7, 9 and 11 mm diameters by CFD simulation.	135
4.9	Comparisons of measured and predicted pressure distribution along the jet for 3 mm diameter nozzle	136
4.10	Comparisons of measured and predicted pressure distribution along the jet for 5 mm diameter nozzle	136
4.11	Comparisons of measured and predicted pressure distribution along the jet for 7 mm diameter nozzle	137
4.12	Pressure decay against distance for nozzle with diameters of 3, 5 and 7 mm	137
4.13	Force decay against distance for orifice with diameters of 3, 5 and 7 mm	138
4.14	An example of particle size distribution curve from AH1-3	141
4.15	Distribution of sand material within the backfill depth	143
4.16	Dry backfill material	144
4.17	Partly saturated	144
4.18	Grains from sieve test for mineral identification	145
4.19	Images of particles taken from auger hole 1	147
4.20	PSD curve for model backfill material	152
4.21	A comparison of average PSD curve for actual and model backfill materials	154
4.22	Specimen surface after (a) nozzle and (b) orifice jetting impact of 5 mm diameter	156
4.23	Nozzle (5 mm) jetting impact upon specimen	158
4.24	Orifice (5 mm) jetting impact upon specimen	159
4.25	Thickness reduction for 5 mm orifice jetting	162
4.26	Thickness reduction for 5 mm nozzle jetting	163
4.27	Thickness reduction for lines A1, C1 and E1	165
4.28	Thickness reduction for lines B2 and D2	166
4.29	Thickness reduction for lines A3, C3 and C3	167
4.30	Thickness reduction for lines B4 and D4	168
4.31	Thickness reduction for lines A5, C5 and E5	169
4.32	Mapping of erosion region	170

4.33	Thinning rate ($mm/hr \times 10^{-5}$) according to data taking template for orifice jetting	174
4.34	Thinning rate ($mm/hr \times 10^{-5}$) according to data taking template for nozzle jetting	175
4.35	Close-up of the rupture point for 5 mm orifice jetting	176
4.36	Close-up view of the effect of sand particle size for 3 mm jetting hole on sand and water wall shear	179
4.37	A comparison of experimental and simulated results	180
4.38	CFD results on effect of sand particle size for 5 mm jetting hole on sand wall shear and velocity	181
4.39	CFD results on effect of sand compactness for 5 mm jetting hole on wall shear and velocity for sand and water	183
4.40	CFD simulated results of sand wall shear for 5 mm jetting hole at 200, 300 and 400 mm separation distance	185
4.41	CFD simulated results for water wall shear of 5 mm jetting hole at 200, 300 and 400 mm separation distance	186
4.42	CFD simulated results of sand and water velocity of 5 mm jetting hole at 200, 300 and 400 mm separation distance	188
4.43	CFD simulated results on sand and water velocity at 400 mm separation distance for 1, 3, 5, and 7 mm jetting hole	189
4.44	A comparison of the experimental finding and CFD simulation results	191

LIST OF ABBREVIATIONS

SCADA	-	Supervisory Control and Data Acquisition System
CFD	-	Computational Fluid Dynamics
NPS	-	Nominal Pipe Size
SEM	-	Scanning Electron Microscopy
ASTM	-	American Standard Technical Material
ISO	-	International Organisation for Standardisation
API	-	American Petroleum Institute
PGU	-	Peninsula Gas Utilisation Project
BSCFD	-	Billion Standard Cubic Feet Day
GMB	-	Gas Malaysia Berhad
AISI	-	American Iron and Steel Institute
JIS	-	Japanese Industrial Standard
ASME	-	American Society of Mechanical Engineers
AASTHO	-	American Association of State Highway Transportation Officials
PSD	-	Particle Size Distribution
MS	-	Malaysian Standard
LNG	-	Liquefied Natural Gas
RGT	-	Regasification Terminal
NG	-	Natural Gas
LPG	-	Liquefied Petroleum Gas
MDPE	-	Medium Density Polyethylene
NPS	-	National Pipe Standard
UPVC	-	Unplasticised Polyvinyl Chloride
SPQ	-	Spike Parameter Quadratic
SP	-	Spike Parameter
EN	-	European Standard

PSD	-	Particle Size Distribution
NSE	-	Navier-Stokes Equation
RSN	-	Reynold Stress Model
SST	-	Shear Stress Transport
CRC	-	Corrosion Research Centre
DEM	-	Discrete Element Method

LIST OF SYMBOLS

α	-	Impaction angle
r	-	Radius
θ	-	Angle of particle rotation
C_D	-	Drag coefficient
d_p	-	Particle diameter
g	-	Gravitational acceleration
k	-	Fluid turbulent kinetic energy
k_1	-	Erosion model constant
L_s	-	Characteristic length
m	-	Particle mass
n	-	Erosion model constant
p	-	Fluid pressure
r_f	-	Fluid phase volume fraction
r_p	-	Particulate phase volume fraction
S_i	-	Stokes number
u_f	-	Fluid velocity
u_p	-	Particle velocity
V_R	-	particle relative velocity
V_I	-	Particle impact velocity
V_s	-	Characteristic velocity
β	-	Particle mass loading
ε	-	Fluid turbulence dissipation rate
γ_I	-	Particle impact angle
μ_{eff}	-	Effective viscosity for fluid phase
μ_f	-	Fluid dynamic viscosity
ρ_f	-	Fluid density
ρ_p	-	Particle density

d_p	-	Particle size
ER	-	Erosion ratio
F_D	-	Drag force per unit particle mass
F_s	-	Sharpness factor
L	-	Flow characteristic length
n	-	Velocity exponent constant
Re	-	Reynolds number
St	-	Stokes number
U	-	Fluid velocity
V_{Jet}	-	Averaged jet exit velocity
V_p	-	Particle impact velocity
Δh	-	Erosion depth
θ	-	Jet impingement angle
μ	-	Fluid viscosity
ρ_p	-	Particle density
ρ_w	-	Target wall density
τ	-	Relaxation time of the particle
d_m	-	Mean particle diameter
E_L	-	Linear material removal rate
h	-	Step height
k	-	Kinetic energy of turbulence
p	-	pressure
\bar{U}	-	Free-stream velocity
v	-	Impact velocity
ρ_p	-	Particle density
a, b	-	Exponent constants
A_i	-	Impact angle empirical constant
C_μ	-	Turbulence model constant
d_p	-	Particle diameter
D	-	Pipe diameter
d_0	-	Threshold particle diameter below which no erosion occurs
d'	-	Standard particle diameter
e	-	Coefficient of restitution
e_n	-	Restitution coefficients in normal direction

e_t	-	Restitution coefficients in tangential direction
E_p	-	Elastic modulus of particle
E_t	-	Elastic modulus of target
E_e	-	Effective elastic modulus
F_S	-	Particle shape factor
F_P	-	Pressure gradient force
F_e	-	Specific erosion factor
F_P	-	Penetration factor
F_M	-	Empirical constant accounting for material hardness
g	-	Gravity acceleration
H_p	-	Hardness of particle
H_t	-	Hardness of target
H_V	-	Vickers hardness of target
K_c	-	Fracture toughness
K_p	-	Physical characteristics constant
K_s	-	Fitting erosion constant
K_T	-	Kinetic energy transferred from impacting particle to target per unit mass of particles
l_e	-	Eddy length scale
L	-	Depth of deformation
L_V	-	Plastic zone volume
L_{stag}	-	Stagnation region length
L_{ref}	-	Reference length
L_S	-	Slug body length
L_F	-	Liquid film length
m_p	-	Mass of single particle
\dot{m}	-	Sand mass ratio in slug body
n_h	-	Strain hardening exponent
n_p	-	Physical characteristics constant
n_s	-	Shape constant
\bar{p}	-	Mean stress
p_n	-	Normal pressure component
p_t	-	Tangential pressure component
P	-	Constant plastic flow stress

r	-	Radius of particle
R	-	Roundness of particle
r_c	-	Bend radius of curvature
Re_p	-	Particle Reynolds number
Re_L	-	Liquid Reynolds numbers
t_e	-	Eddy time scale
T_{int}	-	Particle eddy interaction time
t_{life}	-	Eddy life time
t_{cross}	-	Particle eddy cross time
V_{char}	-	Flow characteristic velocity
V_e	-	Erosional velocity
V_m	-	Mixture velocity
V_p	-	Particle velocity
V_{pn}	-	Normal velocity component of particle
V_{pt}	-	Tangential velocity component of particle
V_r	-	Residual parallel component of particle velocity at small angles of attack
V_θ	-	Threshold velocity below which distortion is entirely elastic and no damage occurs
\dot{W}_p	-	Sand flow rate
x_t	-	Horizontal coordinate
δ	-	Deformation wear factor, the amount of energy needed to remove unit volume of material
σ^*	-	Pressure-stress ratio
ψ	-	Ratio of depth of contact to depth of cut
ε	-	Turbulent dissipation rate
τ	-	Particle relaxation time
B	-	Brinell hardness
B_F	-	Body force
B_w	-	Stiffness ratio
b, I	-	Function of material's properties
C_k	-	Cutting characteristic velocity
$C(d_p)$	-	Function of particle diameter
C_μ	-	Turbulent model constant
D_p	-	Particle diameter

D_K	-	Deformation characteristic velocity
d	-	Maximum crater diameter
$\frac{dKEsPD}{dt}$	-	Particle kinetic energy
E	-	Young's modulus
E_f	-	Empirical constant specifying the energy required to remove a unit volume of the target material by deformation wear
E_r	-	Reduced Young's modulus of elastically
E_t	-	Modulus elasticity of target material
E_p	-	Modulus elasticity of the particles
E_{pd}	-	Erosion rate for the power dissipation model
E_{sp}	-	Specific energy
e	-	Rebounding coefficient
$f(\alpha)$	-	Function of impact angle
G_k	-	Generation of turbulent kinetic energy
H	-	Depth of bury parallel pipe
H_{vs}	-	Vickers hardness
K_A	-	Shape factor
K_F	-	Ratio of vertical to horizontal (frictional) force
K_{NG}	-	Velocity component normal to the surface below which no erosion takes place in certain hard material
k	-	Turbulence energy
k_c	-	Constant determined by the material properties of particle and target
M	-	Total mass of abrasive Particles
M_p	-	Mass of impacting Particle
n	-	Empirical coefficient
n_F	-	Velocity exponent
n_L	-	Velocity exponent for metallic materials
n_{NG}	-	Empirical constant
n_h	-	Shape factor of impingement particles and charges in a range of 0.5 (line cutting) - 1 (area cutting)
P	-	Constant pressure (analogous to the quasi-static

		indentation hardness)
P_A	-	Yield pressure during the impact
P_E	-	Eroding target material pressure
P_{PD}	-	Power dissipation
P_t	-	Tangential pressure during cutting process
P_n	-	Normal cutting pressures during cutting process
Q_f	-	Particle mass flux
q	-	Quartz
β_0	-	Angle of maximum erosion
β_l	-	Relative angle between particle path and specimen surface
γ	-	Soil weight
φ	-	Soil friction angle of the trench wall
ε	-	Dissipation rate
ε_B	-	Hardness of the target material
ε_b	-	Deformation wear factor
ε_0, σ_B	-	Elongation of target material
ε_d	-	Energy needed to remove a unit volume of material from a body due to deformation wear
σ	-	Yield strength
σ_k	-	Turbulent Prandtl numbers for turbulent energy
σ_ε	-	Turbulent Prandtl numbers for dissipation rate
σ_y	-	Elastic load limit Energy needed to remove a unit volume of material from a body due to cutting wear
ρ_t	-	Target material density
μ	-	Dynamic viscosity
μ_C	-	Friction coefficient
μ_T	-	Turbulent viscosity
ε_C	-	Critical strain
δ	-	Kronecker-Delta function
q_p	-	Particles Poisson's ratio
q_t	-	Target material Poisson's ratio
R_f	-	Particle roundness factor Tangential restitution ratio
r_s	-	Radius particle corresponding to the sphere

r_p	-	Radius of impacting Particle
S_t	-	Stiffness of the target material
S_p	-	Stiffness of the Particle
u	-	Fluctuating velocity due to turbulence
V	-	Velocity
V_C	-	Critical impact velocity
V_{el}	-	Threshold velocity (the velocity of collision at which the elastic limit of eroding surface is just reached)
V_f	-	Volume of fluid
V_n	-	Normal impact velocity
V_p	-	Particle velocity
W	-	Total volume of target material removed
W_c	-	Cutting wear
W_d	-	Deformation wear

Subscript

c	-	Centre line
p	-	Pipe
r	-	Radial
z	-	Vertical
Amb	-	Ambient
Avg	-	Average
Min	-	Minimum
Max	-	Maximum
t	-	Turbulence

LIST OF APPENDICES

APPENDIX	TITLE	PAGE
A.1	The schematic diagram of the overall experimental rig construction	211
A.2	Water pump structure and piping system	212
A.3	Configuration of experimental rig design	213
B.1	Calibration of digital thickness gauge	214
B.2	Calibration of Ashcroft pressure gauge	216
C.1	Particle size distribution for auger AH 1-1	217
C.2	Particle size distribution for auger AH 1-2	218
C.3	Particle size distribution for auger AH 1-3	219
C.4	Particle size distribution for auger AH 1-4	220
C.5	Particle size distribution for auger AH 2-1	221
C.6	Particle size distribution for auger AH 2-2	222
C.7	Particle size distribution for auger AH 2-3	223
D.1	Particle shape calculation for sample AH 1-1	224
D.2	Particle shape calculation for sample AH 1-4	225
D.3	Particle shape calculation for sample AH 1-2	225
D.4	Particle shape calculation for sample AH 2-1	226
D.5	Particle shape calculation for sample AH 1-3	226
D.6	Particle shape calculation for sample AH 2-2	227
D.7	Particle shape calculation for sample AH 2-3	227
E.1	Sieve test for sample sand 1	228
E.2	Sieve test for sample sand 2	229
E.3	Sieve test for sample sand 3	230
F.1	Thickness reduction data for orifice jetting	231
F.2	Thickness reduction data for nozzle jetting	232

G.1	CFD results on effect of Jetting hole (1, 3, 5 and 7 mm) on sand and water wall stress	233
G.2	CFD results on effect of sand particle size for 3 mm jetting hole on wall shear stress and velocity of sand and water	234
G.3	CFD results on effect of sand particle size for 5 mm jetting hole on wall shear stress and velocity of sand and water	235
G.4	CFD results on effect of sand compactness for 3 mm jetting hole on wall shear and velocity for sand and water	236
G.5	CFD results on effect of sand compactness for 5 mm jetting hole on wall shear and velocity for sand and water	237
G.6	CFD results on effect of separation distance for 1 and 3 mm jetting hole on sand and water wall shear	238
G.7	CFD results on effect of separation distance for 5 and 7 mm jetting hole on sand and water wall shear	239

CHAPTER 1

INTRODUCTION

1.1 Background and Motivation

Natural gas is well known as the cleanest of all fossil fuels and highly efficient form of energy. Plentiful of supply and competitive cost of natural gas offers great advantage to become a prominent fuel used in either commercial or industrial. Pipeline systems covers a wide range of span from the production fields to the gas processing plants and finally to the end users. Natural gas is transported from gas processing plant to its users through a stretch of pipeline system. Natural gas is delivered directly to homes and business communities through local distribution lines via distribution gas utility companies. Therefore, gas transportation and distribution play significant role for the development of energy resource. In ensuring continuous supply of natural gas to residential, commercial and industrial area, natural gas pipeline is built with high integrity in ensuring the security of supply [1].

Natural gas is typically transported through buried pipeline. Natural gas distribution pipeline is commonly laid side-by-side with other utilities such as; water pipeline, electrical and telecommunication cables. Most utility system commonly found to be laid within a similar vicinity of natural gas pipe system is water pipeline. Failure of high pressurised

water pipeline normally produced erosive slurry jetting towards adjacent utilities. It might be due to material failure and poor jointing installation.

Water jet impact can exert enough forces upon any surface resulting to its subsequent physical penetration. Currently, mechanical cutting of materials using blades is being replaced with water cutting, using the principle of water jet. Water jet alone might not be able to contribute major degradation upon any surface, but with the presence of solid particle in the jet stream would result to a significant physical damage and might pose bigger threat to the gas pipeline. Failures due to the degradation of pipeline material could seriously disrupt supply continuity and pose threat to life and surrounding environment. Cases of natural gas pipeline failures have proven to be catastrophic as reported by National Transportation Safety Board. The most common reasons for such failures are from external interferences, corrosion, poor construction activities and erosion by erosivity slurries [2-5].

Erosive wear is a phenomenon of metal degradation due to the repetitive impaction of solid particles entrained in a moving fluid onto any surfaces that directly causes material losses [6]. Slurry erosion which is formed by the interaction of solid particles suspended in liquid media with metal surface could easily trigger losses of mass through repeated impacts of particles [7]. This type of erosion has been reported as one of the main sources of failure of many engineering equipment such as slurry pumps, control valves, actuators, accumulator, pipes, tubes and hoses [8-12]. This erosive slurry impact may cause serious metal thinning and finally lead to operational failures of pressurised natural gas pipes. This event could initiate much disastrous incidence especially to those involving escape of flammable gases [2-5]. Pipe was manufactured, hydrostatically tested and coated according to international standards such as API 5L Grade B, ASTM A106 and ISO 3183 to diminish possibility of material and manufacturing defects.

With the advancement in the pipe manufacturing technology, manufacturing defects could drastically reduce. Pipeline protections using appropriate pipe coating and cathodic protection system, coupled with good constructions practices, may boost the integrity of pipeline with longer operational services, whose life-span is estimated within

20 to 30 years [13]. Despite the advances in natural gas pipe manufacturing, effective construction management strategy, stringent testing procedures and thorough quality inspection, failure does occasionally occur. Over half of all in-service pipelines failures have been resulted from some externally applied mechanical force towards the pipes [14]. Mechanical damages such as gouge and dent, fatigue cracking, corrosion, and stress-corrosion cracking are among popular root cause for pipes failures [14]. Materials defects are non-common causes of service failures because they often revealed their quantities prior to placing in service, either during physical inspection of the pipe or during high pressure hydrostatic testing.

Pipeline failures were progressively reported mainly due to explosion, sandblasting and cracks [15-22]. Material degradation caused by corrosion was identified as the main contributing factor to the failure of the pipe. They were apparent based on published reports by Hernandez [23], Rodriguez [24], Shi [25] and Al-Owaisi [26]. Another common caused in pipeline failure is ductile fracture as was reported by Zhang [27]. Whereas Majid et al. [28] reported that the root cause of the buried pipeline leak was due to continuous impact mode by the erosive slurries (a mixture of an insoluble substance in a liquid) from leaked water pipe mixed with the surrounding erosive soil.

Historical data have shown that serious accidents involving natural gas pipeline are considerably rare in nature compared to road accidents, yet they often cause more severe implication to the society [29-32]. The impact of this mishap always relates to the loss of life and structures [2-5]. These scales of event have driven intensive research efforts to formulate preventive measures towards predicting, overcoming and quantify these incidents. Diverse disciplines of research have been enlisted to tackle these issues. Many efforts and methods have been applied in order to identify the impacts [33-37], estimate the risks [38-42], analyse the system reliability [43-45], establish the safety distances from pipeline facilities [30 & 46] as well as other relevant studies that have been conducted with regards to pipeline accident [47].

Since corrosion has been recorded as the major cause of pipeline failure [2-5], less attention was given on the aspect of possible danger that could be created by water pipeline

leakage positioned adjacent to the operational gas pipe system. In the presence of water, sands granules (typically employed as part of backfilling material) can easily form slurries. Continuous impaction has proven to cause severe metal losses and metal thinning which eventually leads to pipeline failure [11, 12, 28].

Haklar and Dresnack [47] studied and proposed standardised safe separation distance (above ground) at which pipelines can be safely assigned from the community arrangement by determining the heat flux, mass release rate from the ruptured pipe and the flame height of the ignited gas. Study carried out by Sklavounos and Rigas [30] focused on estimating the safety distances for liquefied petroleum gas and natural gas pipelines, based on possible outcomes of an accident associated with fuel gas released from pressurised distribution piping system. To date, the study on safety distance is only limited to the explosion of above ground pressurised transmission system. Although this is a common concern among industrial players and government agencies, it should be noted that similar phenomenon can also trigger serious threats to underground pipes by silent yet destructive trail. ASME B31.8 stipulated 152 mm for gas pipeline to any structures whereas Institution of Gas Engineers under their technical directive applied 250 mm safety distance. Experimental study is the best method to understand and establish the relationship between various parameters on the subject being studied. With the established experimental data and appropriate validation, computer simulation can be employed to reduce the cost and time taken for full scale experimental investigations.

Computer simulation is an effective method that complements the experimental techniques. It is in a form of controlled computational experiments which allow various parameters to be studied separately under various conditions within stipulated boundary. Additionally, model generated by simulation process could provide details insight in understanding the dynamic behaviour of various engineering problems, thus drawing appropriate preventive design measures. The use of this method by many researchers proven to shows good agreement with what was presented by analytical techniques [48-50]. A prediction of pipeline failure through computer simulation is proven to be an effective method to optimise the design of pipes and their operating conditions. Study by Yang [51] on the failure analyses of a piping system in hydro processing reactor effluent air cooler showed that the analytical results are having similar trends with the actual failure

instances, whereas study by Moustabchir and Alhussein [52-53], proved that numerical calculations are a reliable technique by showing acceptable coincidence with the actual failed specimen.

In the present study, the experimental study was conducted with the aims of shedding some light on the effect of erosive jetting upon an impacted surface thus allowing a better understanding on the prevention technique to be deployed for the existing natural gas pipeline sharing the similar trench with water utility pipeline. At present, the typical construction approach of similar sort employs a separation distance at the minimum of 300 mm horizontally away from surface curvature tip [56]. It is imperative that this distance be scrutinised in ensuring sufficient distance to minimise or curbing the effect of erosive jetting by performing this experiment.

In this particular work, a newly designed experimental rig was developed to facilitate the experimental exercise that may represent the actual condition of erosion study of the failed natural gas piping system at site. The study is considered as a unique attempt to study erosion of buried pipe in slurry environment. This rig can also be employed for the extended study in different mixing environment of water-sand proportion and at elevated jetting pressure. The water jetting characteristics and pressure decay curve in water-water, water-air and water-sand environment were established and can be used as an initial guide for further study in determining the separation distance for other pipeline configurations.

1.2 Problem Statement

In late September of 2004, a natural gas pipeline leak was identified. This gas pipe failure was categorized as a gas distribution system which was located within industrial community customers. The continuous bubbling gas through water-logged soil was just like a sounding alarm of gas pipe leak. Ruptured pipe at incident location was evident after excavation as shown in Figure 1.1a. Figure 1.1b shows the ruptured natural gas pipe. It

was discovered that there were three pipes; DN200 API 5L X42 carbon steel and a 125 mm medium density polyethylene (MDPE) natural gas pipes, and 152 mm asbestos water pipe lying parallel to each other were directly affected, with all three indicating signs of serious damage or leakage. An electrical cable lying parallel to the pipes slightly at a high elevation indicates no apparent sign of damage. Figure 1.2 shows the pipeline layout at the location of incident.



(a) Ruptured pipes at incident site

(b) Closed-up view of natural gas pipe

Figure 1.1 Arrangement of failed pipes

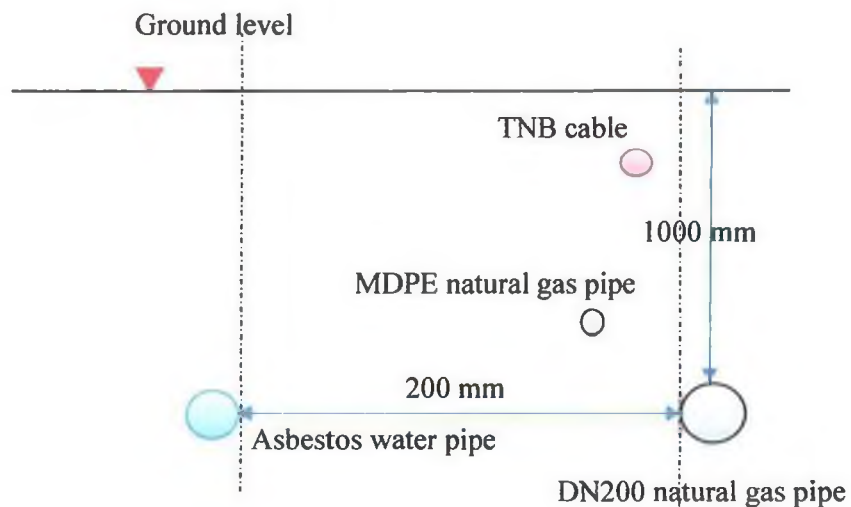


Figure 1.2 Pipeline layouts

The API 5L X42 carbon steel with a nominal pipe size of 203 mm and MDPE pipe was carrying 1,800 kPa and 345 kPa natural gas, respectively, prior to shut down. The 152 mm, asbestos pipe was transporting water with an estimating flowing pressure of 1,000 kPa. The DN200 natural gas pipe is made of carbon steel manufactured with stringent specification of API 5L X42. It was buried around 1000 mm below the ground level at about 200 mm laterally from the underground water pipe (surface to surface distance). Roughly with a shorter distance between the gas and the water pipes is the location of MDPE gas pipe. The established thicknesses of the DN200 pipe, MDPE and asbestos pipe were 5.6 mm, 11.4 mm and 10 mm, respectively.

Water pipelines are normally designed and work at high pressure level for more than 500 kPa. These sorts of facilities are in fact a common typical feature laid in the vicinity of natural gas pipes that may pose severe threat due their probabilities of failures. Water might be considered as non-hazardous material to our environment and usually any leakages was not entertained at once. Failure of water pipeline will normally start with small slit and the size will enlarge until it reaches the bursting stage. The initial leak will form high pressure water jetting. A leak of high pressure water pipe in a mixture of soil and sand could create erosive slurry impaction on nearby pipes. Slurry erosion is usually formed by the interaction of solid particles suspended in liquid with a surface that experiences losses of mass by repeated impacts of particles entrained in moving liquid.

They are many factors that influence the erosion effect on the external surface of buried pipelines. Finnie [54] has identified and classified it into three categories; first, particle flow conditions such as particle velocity, particle rotation and angle of impingement. Secondly, properties of the slurries which is soil hardness, angularity, shape, and strength. Lastly the properties of target material, such as surface hardness, topography, ductility and other mechanical properties. The actual effect of these factors is still dubious due to its physical arrangement complexity and unpredictable nature at buried pipelines conditions. Thus, it is imperative for this study to be carried out in order to understand the hydrodynamic characteristics of water jetting to understand the effect of water jet diameters, sand particle size and separation distance upon the erosion of natural gas pipe. This study is the first ever conducted to understand the erosion effect on external surface

of buried natural gas pipeline. Previous erosion study by other researches are mainly focusing on internal surface of pipeline [15, 29, 54].

1.3 Research Hypothesis

Erosion of external surface of buried pipelines in slurry environment is very much influenced by the slurry properties as well as the pressure of the carrier medium. Since the backfilling materials are mainly soil with sand the presence of various sand size with irregular edges will significantly affect erosion rate. Furthermore, the higher the pressure of the carrier medium the higher the impaction pressure thus causes high velocity region around the stagnation point. It is expected that the formation of the impact area will be in form of less eroded smooth surface zone at the centre of impaction will be surrounded by highly eroded rough surface region. It is also expected that the thinning rate and stand-off or zero effect distance will be lesser as the source of impact is located further from the jetting source. The thinning rate of specimen will also be expected to vary with an increase of time scale.

1.4 Objectives

The aim of this study is to assess the buried natural gas distribution pipeline integrity in close vicinity with the adjacent water piping utilities. Specific objectives include the following:

- (a) To characterize the backfilling materials used in underground natural gas pipeline installation.

- (b) To experimentally evaluate the effect of water leakage in a slurry environment on the erosion characteristics of natural gas pipeline.
- (c) To computationally evaluate the erosion characteristics of natural gas pipeline.

1.5 Scope of Study

The research was conducted experimentally using DN200 API 5L X42 carbon steel natural gas pipe environment and computationally by conducting Computational Fluid Dynamic (CFD) simulation using Reynold Average Navier-Stokes flow model. The Eularian-Lagrangian particle tracking technique was used to validate the experimental results. In order to accomplish all the objectives, several scopes are outlines, which are:

- i. Identifying the particle size distribution, mineral types and angularity of the backfilling material.
- ii. Variating of jetting sizes at 1, 3, 5, and 7 mm.
- iii. Variating of sand sizes between 0.2 mm to 2 mm.
- iv. Fixing the jetting distance at 200, 300, and 400 mm.
- v. Variation of soil compactness of 90%, 70% and 50% was used to imitate typical condition of buried pipe.

1.6 Limitation of Study

This research involves experimental and numerical studies on the erosion of natural gas pipe due to the impaction of erosive slurry formed by the induction of high pressure water jet onto the surface of high pressure natural gas pipe. The best suited condition of

preparing a similar buried pipe environment used in the experimental study is limited to the following constraints:

- i. Pipe material of only type DN200 API 5L X42 to simulate the actual specimen in the case study.
- ii. Test pipe contains no pressurised gas.
- iii. Coating condition is as received and supplied from the mill (organic paint of 3.76×10^{-6} m thickness).
- iv. Water jet supply pressure was fixed at 1000 kPa.
- v. Jetting angle was positioned at 90° (horizontal position).
- vi. Jetting source is from nozzle and orifice type of outlet induced leakage.
- vii. The pipe is use for class location 4 (pipe thickness: 5.6 mm).
- viii. No corrosion effect will be considered.
- ix. Computational domain of 2815 mm, 1220 mm and 810 mm for long, height and wide respectively.
- x. Inlet and outlet pressure were at 1013 atm and 103 atm.
- xi. Standards $k-\epsilon$ turbulence model.
- xii. Eularian-Lagrangian model for the particle tracking.
- xiii. Discrete phase model for velocity tracking.

1.7 Significance of the Study

A common practice in the natural gas distribution pipeline system is that the designated trench is usually located side-by-side with other utility system such as water utility pipeline and electricity utility cabling due to limited spacing availability or congested nature of the area. To lay a natural gas pipeline next to an electricity utility could pose higher threats of explosion should there be cases of gas leakage. Therefore, laying the gas pipeline next to the water utility pipeline would be the solution as water is considered as non-ignited source to initiate ignition. However, as the water pipe leaks, high pressure water is typically triggered, coupled with surrounding sand and soil, highly erosive slurries

usually be formed. The impaction of this slurries may cause severe metal losses and metal thinning of the impacted pipes which eventually lead to its failure.

1.8 Thesis Organisation

This thesis describes the erosion of carbon steel gas pipe due to high pressure water jetting in erosive slurry environment. Although much knowledge has already been acquired in solid particle impaction on flat surface material. Considerable amount of understanding is very much limited to emulate actual surrounding environment using experimental and numerical studies. In view of its significance, this thesis outlined the documented structure of experimental and numerical approach on the erosion of DN200 API 5L X42 carbon steel natural gas pipeline due to high pressure water jetting in erosive slurry environment.

Chapter 1 provides a general preface of pipeline erosion and its effect on safety of the gas distribution system. Series of reported pipeline failures urged the need to study to the erosion behaviour with respect to the effect of backfilling soil properties and jetting pressure. The chapter also presents the background, problem statement, objectives, scopes, limitations of the study, significant of the study and thesis organisation. The thesis has been divided into five chapters with seven appendices.

Chapter 2 provides the overall review on previous works related to similar issues of research findings on erosive wear due to slurry erosion. Literature review was designed to provide a summary of the available knowledge involving the issues of interest. It presents the research works on erosive wear and its major influencing factors, effect of slurry erosion on ductile materials and CFD simulation study in erosive wear of pipeline surface by various investigators.

Chapter 3 explains the research methodology in two different sections. It includes a detailed description of the experimental activities and simulation sequences. This chapter details out the experimental activities that will include the study of backfilling soil, jet dispersion and water jetting erosion experiments. Finally, this chapter will highlight the employed CFD simulation study to establish erosion morphology on the surface of pipeline.

Chapter 4 presents the detailed discussion of the results obtained on the jet dispersion study and erosion morphology analyses for both experimental and numerical simulation on pipeline due to high pressure jet using selected sand particle sizes that was pre-determined from the incident site.

Chapter 5 provides overall conclusion of research conducted and accommodate recommendations for future undertakings.

REFERENCES

1. API SPEC 5L, Specification for Line Pipe, *American Petroleum Institute*, Dallas, TX.
2. National Transportation Safety Board. *Pipeline Incident Report, Natural Gas Pipeline Rupture and Fire during Dredging of Tiger Pass, Louisiana, 1996*. Virginia: National Technical Information Service; 1997. (NTSB; USA, 2003.
3. National Transportation Safety Board. *Pipeline incident report, Natural gas pipeline rupture and subsequent explosion at St. Cloud, Minnesota, 1996*. Virginia: National Technical Information Service; 1998.
4. National Transportation Safety Board. *Pipeline Incident Report, Natural Gas Pipeline Rupture and Fire in South Riding, July 1998*. Virginia: National Technical Information Service; 2001.
5. National Transportation Safety Board. *Pipeline Incident Report, Natural Gas Pipeline Rupture and Fire, Near Carlsbad, New Mexico, August 2000*. Virginia: National Technical Information Service; 2003.
6. Hutchings. I. M. Particle Erosion of Ductile Metals: A Mechanism of Material Removal. *Wear*, 1974. 27: 121-128.
7. Al-Bukhaiti. M. A., Ahmed. S. M., Badrul. F. M. F. and Emar. K. M. Effect of Impingement Angle on Slurry Erosion Behaviour and Mechanisms of 1017 and High-Chromium White Cast Iron. *Wear*, 2007. 262: 1187-1198.
8. Hamzah. R., Stephenson. D. J. and Strutt. J. E. Erosion of Materials Used in Petroleum Production. *Wear*, 2004. 186: 493-496.
9. Llewellyn. R. J., Tick. S. K. and Dolman. K. F. Scouring Erosion Resistance of Metallic Materials used in Slurry Pump Service. *Wear*, 2004. 256: 592-599.
10. Aiming. F., Jinming. L. and Ziyun. T. Failure Analysis of the Impeller of Slurry Pump Subjected to Corrosive Wear. *Wear*, 1995. 181-182(2): 876-882.

11. Haugen. K., Kvernfold. O., Ronold. A., and Sandberg. R. Sand Erosion of Wear-Resistance Materials: Erosion in Choke. *Wear*, 1995. 186: 179-188.
12. Al-Bukhaiti, M. A., Ahmed, S. M., Badran, F. M. F., and Emara, K. M. Slurry Erosion Parameters-a Review, in: *The 3rd Assiut University Int. Conf. on Mech. Eng. Advanced Tech. for Ind. Application, Assiut, Egypt*. June 20-23, 2006. Assiut, Egypt, 2006. 210-219.
13. Hassan. F. and Iqbal. J. Consequential Rupture of Gas Pipeline. *Engineering Failure Analysis*, 2006. 3: 127-135
14. Gledon. D. N. and Smith. R. B. An Analysis of Reportable Incidents Natural Gas Transmission and Gathering Lines 1970 through 1978; *NG-18 Report No. 121*. Sept. 1980: 25-35.
15. Peekema. R. M. Causes of Natural Gas Pipeline Explosive Ruptures. *Journal of Pipeline System Engineering and Practice*, 2013. 4: 74-80.
16. Hassan. F. and Iqbal. J. Consequential Rupture of Gas Pipeline. *Engineering Failure Analysis*, 2006. 3:127-135.
17. Hassan, F. Iqbal, J. and Ahmed, F. Stress Corrosion Failure of High-Pressure Gas Pipeline. *Engineering Failure Analysis*, 2007. 14: 801-809.
18. Azevedo. C.R.F. Failure Analysis of a Crude Oil Pipeline. *Engineering Failure Analysis*, 2007. 14: 978-994.
19. Shalaby. H.M., Riad. W.T., Alhazza. A.A., Behbehani. M, H., Failure Analysis of Fuel Supply Pipeline. *Engineering Failure Analysis*, 2006. 13:789-796.
20. Kumar. M.S., Sujata. M., Venkataswamy. M.A., Bhaumik. S.K. Failures Analysis of Stainless Steel Pipeline. *Engineering Failure Analysis*, 2008. 15:497-504.
21. Ashrafizadeh. H., Karimi. M., Ashrafizadeh. F. Failure Analysis of a High Pressure Natural Gas Pipe Split Tee by Computer Simulations and Metallurgical Assessment. *Engineering Failure Analysis*, 2013. 32: 188-201.
22. Zhao. Y., and Song. M. Failure Analysis of a Natural Gas Pipeline. *Engineering Failure Analysis*, 2016. 63: 61-71.
23. Hernandez-Rodriguez. M.A.L., Martinez-Delgado. D., Gonzalez. R, Perez Unzueta. A, Mercado-Solis. R.D., Rodriguez. J. Corrosive Wear Failure Analysis in A Natural Gas Pipeline. *Wear*, 2007. 263: 567-71.
24. Rodriguez. H., Delgado. M., Gonzalez. R., Enzeta. P., Solis. M., and Rodriguez. J. Corrosive Wear Failure Analysis in A Natural Gas Pipeline. *Wear*, 2007. 263:567-571.

25. Shi. L., Wang. C., and Zou. C. Corrosion failure of L485 Natural Gas Pipeline in CO₂ Environment. *Engineering Failure Analysis*, 2014. 36: 372-378.
26. Al-Owaisi. S.S., Becker. A. A., and Sun. W. Analysis of Shape and Location Effects of Closely Spaced Metal Loss Defects in Pressurised Pipes. *Engineering Failure Analysis*, 68; 2016; 172-186.
27. Zhang, B., Ye, C., Liang, B. Ductile Failure Analysis and Crack Behavior of X65 Buried Pipes Using Extended Finite Element Method. *Engineering Failure Analysis*, 2014. 45: 26-40
28. Majid. Z.A., Mohsin. R., Yaacob. Z., Hassan. Z. Failure Analysis of Natural Gas Pipe. *Engineering Failure Analysis*, 2010. 17: 818-837.
29. Papadakis. G. A. Major hazard pipelines: A Comparative Study of Onshore Transmission Accidents. *Journal of Loss Prevention in the Process Industries*, 1999. 12: 91-107.
30. Sklavounos. S. and Rigas. F. Estimation of Safety Distance in The Vicinity of Fuel Gas Pipelines. *Journal of Loss Prevention in the Process Industries*, 2006. 19: 24-31.
31. National Transportation Safety Board. *Pipeline Accident no. DCA-99-MP-004*. National Technical Information Service. Virginia US. 2000.
32. Bartenev. A. M., Gelfand. B. E., Makhviladze. G. M. and Robert. J. P. Statistical Analysis of Accidents on the Middle Asia-Centre Gas Pipelines. *Journal of Hazardous Materials*, 1996. 46: 57-69.
33. Olive-sola. J., Gabarrell. X. and Rieradevall. J. Environmental Impacts of Natural Gas Distribution Networks within Urban Neighbourhoods. *Applied Energy*, 2009. 86: 1915-1924.
34. Zhao, Y., Xihong, L. and Jianbo, L. Analysis on the Diffusion of Dynamic Leakage of Gas Pipeline. *Reliability Engineering and System Safety*, 2007. 92:47-53.
35. Jo. Y. D. and Ahn. B.J. Analysis of Hazard Areas Associated with High-Pressure Natural-Gas Pipelines. *Journal of Loss Prevention in the Process Industries*, 2002. 15: 179-188.
36. Mazzola. A. Thermal interaction analysis in pipeline systems: A case study. *Journal of Loss Prevention in the Process Industries*, 1999. 12: 495-505.
37. Zha. Y., Xihong. L. and Jianbo. L. Analysis on the Diffusion Hazards of Dynamic Leakage of Gas Pipeline. *Reliability Engineering and System Safety*, 2007. 92: 47-53.

38. Han. Z.Y. and Weng. W.G. An Integrated Quantitative Risk Analysis Method for Natural Gas Pipeline Network. *Journal of Loss Prevention in the Process Industries*, 2010. 23: 428-436.
39. Brito. A.J. and De Almeida. A.T. Multi-Attribute Risk Assessment for Risk Ranking of Natural Gas Pipelines. *Reliability Engineering and System Safety*, 2009. 94:187-198.
40. Jo. Y.D. and Crowl. D.A. Individual Risk Analysis of High-Pressure Natural Gas Pipelines. *Journal of Loss Prevention in the Process Industries*, 2008. 21: 589-595.
41. Yuhua. D. and Datao. Y. Estimation of Failure Probability of Oil and Gas Transmission Pipelines by Fuzzy Fault Tree Analysis. *Journal of Loss Prevention in the Process Industries*, 2005. 18: 83-88.
42. Jo. Y.D. and Ahn. B. J. A Method of Quantitative Risk Assessment for Transmission Carrying Natural Gas. *Journal of Hazardous Materials*, 2005. 123(1-2): 1-12.
43. Bodner. A.I., Greenwood. B. W. and Hudson. J.M. Risk Analysis of a Sour Gas Pipeline Using a Personal Computer. *Reliability Engineering and System Safety*, 1990. 30: 455-466.
44. Maes. M.A., Dann. M. and Salama. M.M. Influence of Grade on the Reliability of Corroding Pipelines. *Reliability Engineering and System Safety*, 2008. 93: 447-455.
45. Gerbec. M. A Reliability Analysis of a Natural-Gas Pressure-Regulating Installation. *Reliability Engineering and System Safety*. 2010. 95: 1154-1163.
46. Wilson. J.F. Failure Analysis of a Buried Pipeline Transporting Gas. *Journal of Pipe System and Engineering Practice*, 2012. 3(1): 17-21.
47. Haklar. J.S. and Dresnack. R. Safe Separation Distance from Natural Gas Transmission Pipelines. *Journal Pipeline Safety*, 1999. 1(1); 3-20.
48. ElTobgy. M. S., Ng. E. and Elbestawi. M. A. Finite Element Modelling of Erosive Wear. *International Journal of Machine Tools and Manufacture*, 2005. 45:1137-1346.
49. Wang. Y.F. and Yang. Z.G. Finite Element Model of Erosive Wear on Ductile and Brittle Materials. *Wear*, 2008. 265: 871-878.
50. Hongjun. Z., Guang. F. and Qijun. W. Numerical Investigation of Temperature Distribution in an Eroded Bend Pipe and Prediction of Erosion Reduced Thickness. *The Scientific World Journal*. 2014. Article ID 435679.
51. Tang, P., Yang, Jian., Zheng, J., Wong, I., He, S., Ye, J. and Ou, G. Failure Analysis and Prediction of Pipes Due to The Interaction Between Multiphase Flow and Structure. *Engineering Failure Analysis*. 2009. 16(5): 1749-1756.

52. Moustabchir, H., Azari, Z., Hariri, S. and Dmytrakh, I. Experimental and Numerical Study of Stress-Strain State of Pressurised Cylindrical Shells with External Defects. *Engineering Failure Analysis*, 2010. 17: 506-514.
53. Alhussein. H., Capelle. J., Gilgert. J., Tidu. A., Hariri. S. and Azari. Z. Static, Dynamic and Fatigue Characteristics of the Pipeline API 5L X52 Steel After Sandblasting. *Engineering Failure Analysis*, 2013. 27: 1-15.
54. Finnie. I. Some Reflections on the Past and Future of Erosion. *Wear*, 1995. 186-187: 1-10.
55. Petronas Gas Berhad, *Annual Report 2015 Petronas Gas Berhad*, Kuala Lumpur, 2015.
56. Suruhanjaya Tenaga. *Guidelines on Domestic Gas Piping System*. Kuala Lumpur, 2007.
57. Pipeline and Hazardous Materials Safety Administration US Department of Transport, *Report on Pipeline Failure*. 2011, US DOT.
58. Majid. Z. A. and Mohsin. R., Failure Investigation of Natural Gas Pipeline. *Arabian Journal of Science and Engineering*, 2012. 37: 1083-1088.
59. Majid. Z. A., Mohsin. R. Multiple Failure API 5L X42 Natural Gas Pipeline. *Engineering Failure Analysis*, 2013. 31: 421-429.
60. Rohlf, W., Bieber. M., Ehrenpreis, C., Jorg, J., Sabelberg, E., Kneer, K. Flow Structures and Heat Transfer Characteristics in Arrays of Submerged Laminar Impinging Jets. *Proceedings in Applied Mathematics and Mechanics*. September 16, 2016. Weinheim German: Wiley-Vch GmbH & Co. 2016. 953-956.
61. Rahman. A.B. A Review of Effects of Initial and Boundary Conditions on Turbulent Jets. *WSEAS Transactions on Fluid Mechanics*, 2010. 4(5): 257-275.
62. Swathi Krisna. *Characterization of the Flow-Field in Circular Subsonic Impinging jets*. MSc. Thesis. Delft University of Technology; 2012.
63. Ball. C.G., Fellouah. H., Pollard. A. The Flow Field in Turbulent Round Free Jets. *Progress in Aerospace Sciences*, 2012. 50: 1-26.
64. Davies. A.L., Fisher. M.J., Barrett. M. The Characteristics of The Turbulence in The Mixing Region of a Round Jet. *Journal Fluid Mechanics*, 1963. 15(3): 337-367.
65. Góral. D., Kluza. F., Kozłowicz. K. Assessment of Heat Transfer and Mass Change During Fruits and Vegetables Impingement Pre-Cooling. *International Journal of Food Engineering*, 2009. 10(1) :183-189.

66. Wang. X.K., Niu. G.P., Yuan. S.Q., Zheng J.X., and Tan. S.K. Experimental Investigation on The Mean flow field and Impact Force of a Semiconfined Around Impinging Jet. *Fluid Dynamics Research*, 2015. 47(2): 025501.
67. Zuckerman. N. and Lior. N. Jet Impingement Heat Transfer: Physics, Correlations, and Numerical Modelling. *Advances in Heat Transfer*, 2006. 39: 565-631.
68. Wang. S.S, Cai. L.X., Mao. J.R. Liu. G.W. and Di. J. Surface Ripple and Erosion Rate of Stainless Steel Under Elevated Temperature Erosion by Angular Solid Particles. *Journal of Engineering Tribology*, 2014. 228(2): 187-197.
69. Ergin. E., Jonathan. N., Cameron. N., Scmih. M.O., Volkan. O. Experimental Study of a Round Jet Impinging on a Convex Cylinder. *Materials Science and Technology*, 2007. 18: 1800–1810.
70. New T.H., and Long J. Dynamics of Laminar Circular Jet Impingement Upon Convex Cylinders. *Physics of fluids*, 2015. 27: 024109.
71. Shim. Y.M., Richards. P.J., Sharma. R.N. Turbulent Structures in The Flow of The Plane Jet Impingement on a Circular Cylinder. *Experimental Thermal and Fluid Science*, 2014. 57: 27-39.
72. McDaniel C.S. and Webb B.W. Slot Jet Impingement Heat Transfer from Circular Cylinders. *International Journal of Heat and Mass Transfer*. 2000. 42: 2975-1985.
73. AI-Bukhaiti M.A., Ahmed S.M., Badran, F.M.F.; Emara, K.M.: Effect of Impingement Angle on Slurry Erosion Behaviour and Mechanism of 1017 Steel and High-Chromium White Cast Iron. *Wear*. 2007. 262: 1187–1198.
74. Lindsley B. A., Marder A.R. The Effect of Velocity on The Solid Particle Erosion Rate of Alloy. *Wear*. 1999. 225-229(Part 1): 510–516.
75. Finnie, I. Some Reflection on the Past and The Future of Erosion. *Wear*. 1995. 186-187: 1-10.
76. Hutchings. I. M. Particle Erosion of Ductile Metals: A Mechanism of Material Removal. *Wear*, 1974. 27: 121-128.
77. Bitter. J.P.A. A Study of Erosion Phenomena Part I. *Wear*, 1963. 6-1: 5-21
78. Mostafa. M.D., Kevorkov. A., Jedrzejowski. D., Pugh. P., Medraj. M. Water Impingement Erosion of Deep-Rolled Ti64. *Metals*, 2015. 5: 1462-1486.
79. Stachowiak, G.W. and Batchelor, A.W. Abrasive, Erosive and Cavitation Wear. *Engineering Tribology*. Elsevier B.V. 2006: 201-551.
80. Corrosion Testing Laboratories. Technical Brief; Erosion Corrosion, Newark, Delaware USA. 2010.

81. Hasan. F., Iqbal. J., and Ahmed. F. Consequential Rupture of Gas Pipeline. *Engineering Failure Analysis*, 2006. 13: 127–135.
82. Azevedo. C.R.F. and Sinatora. A. Failure Analysis of a Gas Pipeline. *Engineering Failure Analysis*, 2004. 11(3): 389-400.
83. Clark. H. Mcl. On the Impact Rate and Impact Energy of Particle in a Slurry Erosion Tester. *Wear*, 1991. 147: 165-183.
84. Lynn. R., Wong. K.K., Clark. H.M. On the Particle Size Effect in Slurry Erosion. *Wear*, 1991. 149: 55-71.
85. Dosanjh. S. and Humphrey. A.C. The Influence of Turbulence on The Erosion by A Particle-Laden Fluid Jet. *Wear*, 1985. 102: 309-330.
86. Lapiped. L. and Levy. A. The Halo Effect in the Jet Impingement Solid Particle Erosion Testing of Ductile Metals. *Wear*, 1980. 58: 301-311.
87. Neilson. J. H. and Gilchrist. A. Erosion by Stream of Solid Particle. *Wear*, 1968. 11(2): 111-122.
88. Finnie. I. Erosion of Surfaces by Solid Particles. *Wear*, 1960. 3:87.
89. Bitter JGA. A study of Erosion Phenomena, part II. *Wear*, 1963. 6:169–90.
90. Levy. A.V. The Platelet Mechanism of Erosion of Ductile Metals. *Wear*, 1986. 108:1–21.
91. Levy. A.V., Jee. N., and Yau. P. Erosion of Steels in Coal-Solvent Slurries. *Wear*, 1987. 117:115–27.
92. Levy. A.V., and Yau. P. Erosion of Steels in Liquid Slurries. *Wear*, 1984. 98:163-82.
93. Zu. J.B., Hutchings. I.M., and Burstein. G.T. Design of a Slurry Erosion Test Rig. *Wear*, 1990. 140:331–4.
94. Sugiyama. K., Harada. K., and Hattori. S. Influence of Impact Angle of Solid Particles on Erosion by Slurry Jet. *Wear*, 2008. 265(5–6): 713-720.
95. Nguyen. Q.B., Lim. C.Y.H., Nguyen. V.B., Wan. Y.M., Nai. B., Zhang. Y.W. and Gupta. M. Slurry Erosion Characteristics and Erosion Mechanisms of Stainless Steel *Tribology International*, 2014. 79 (24): 1-7.
96. Zheng. Z.B., Zheng. Y.G., Sun. W.H., and Wang. J, Q. Erosion-Corrosion Of HVOF-Sprayed Fe-Based Amorphous Metallic Coating Under Impingement by A Sand Containing Nacl Solution. *Corrosion Science*, 2013. 76: 337–47.
97. Oka. Y.I., Ohnogi. H., Hosokawa, T. and Matsumura, M. The Impact Angle Dependence of Erosion Damage Caused by Solid Particle Impact. *Wear*, 1997. 203-204: 573-579.

98. Clark. H.Mcl. and Wong. K.K. Impact Angle, Particle Energy and Mass Loss in Erosion by Dilute Slurries. *Wear*, 1995. 186-187: 454-464.
99. Yabuki. A. and Masanobu. M. Theoretical Equation of The Critical Impact Velocity in Solid Particles Impact Erosion. *Wear*, 1999. 233-235: 476-483.
100. Sundrajan. G. The Differential Effect of The Hardness of Metallic Materials on The Erosion and Abrasion Resistance. *Wear*, 1993. 162-164: 772-781.
101. Wada. S. Effects of Hardness and Fracture Toughness of Target Materials and Impact Particles on Erosion of Ceramic Materials. *Key Engineering Material*, 1992. 71: 51-74.
102. Clark. HMcl. and Liewellyn. R. J. Assessment of the Erosion Resistance of Steels Used for Slurry Handling and Transport in Mineral Processing Applications. *Wear*, 1993. 260: 32-44.
103. Misra, A. and Finnie, I. On the size effect in abrasive and erosive wear, *Wear*, 1981, 65: 359-373.
104. Desale, G.R., Gandhi, B.K. and Jain, S.C. Effect of Physical Properties of Solid Particle on Erosion Wear of Ductile Materials. *Proceeding of World Tribology Congress III*, September 12-16, 2005, Washington. WTC2005-63997.
105. Hamblin. M.G. and Stochowiak. G.K. Characterization of Surface Abrasivity and its Relation Two-Body Abrasive Wear. *Wear*, 1997. 206: 69-75.
106. Bahadur S. and Badruddin R. Erodent Particle Characterisation and The Effect of Particle Size and Shape on Erosion. *Wear*, 1990. 138: 189-208.
107. Palasamudram. S. L. and Bahadur. S. Particle Characterization for Angularity and the Effects of Particle Size and Angularity on Erosion in a Fluidized Bed Environment. *Wear*, 1997. 203-204: 455-463.
108. Liebhard, M. and Levy, A. The Effect of Erodent Particle Characteristics on the Erosion of Metals. *Wear*. 1991. 151: 381-390.
109. Burstein. G.T. and Sasaki. K. Effect of Impact Angle on the Slurry Erosion-Corrosion of 304L Stainless Steel. *Wear*, 2000. 240: 80-94.
110. Al-Bukhaiti. M.A., Ahmed. S.M., Badran. F.M.F., Emara. K.M. Effect of Impingement Angle on Slurry Erosion Behavior of 1017 Steel and High-Chromium White Cast Iron. *Wear*, 2007. 262: 1187-1198.
111. Green. G.M, Taggart. R. and Polonis. D.H. Influence of Microstructure on the Erosion of Plain Carbon Steels. *Metallography*, 1981. 14: 191-212.

112. Rodriguez. E., Flores. M., Perez. A., Mercado-Solis. R.D., Gonzalez. R., Rodruguez. J. and Valtierra. S. Erosive Wear by Silica Sand on AISI H13 and 410 Steels. *Wear*, 2009. 267: 2109-2115.
113. Fuyan. L. and Shao. H. The Effect of Impingement Angle on Slurry Erosion. *Wear*, 1991. 141: 278-289.
114. Lopez. D., Congote. J.P., Cano. J.R., Toro. A. and Tschiptschin, A.P. Effect of Particle Velocity and Impact Angle on the Corrosion-Erosion of AISI 304 and AISI 420 Stainless Steels. *Wear*, 2005. 259: 118-124.
115. Harsha. A.P. and Deepak. K.B. Solid Particle Erosion Behaviour of Ferrous and Non-Ferrous Materials and Correlation of Erosion Data with Erosion Models. *Materials and Design*, 2008. 29: 1745-1754.
116. Ashrafizadeh. H. and Ashrafizadeh. F. A Numerical 3D Simulation for Prediction of Wear Caused by Solid Particle Impact. *Wear*, 2012. 276-277: 75-84.
117. ASTM D2321: *Standard Practise for Underground Installation of Thermoplastic Pipe for Sever and Other Gravity-Flow applications*. 2012, ASTM International.
118. ASME B31.8. *Gas Transmission and Distribution Piping Systems*. ASME, New York. 2014.
119. ASTM D2488-90. *Standards Practise for Description and Identification of Soils (Visual Manual Procedure)*. ASTM International, US.
120. Halubec, I. and D'Appolonia, E. Effect of Particle Shape on the Engineering Properties of Granular Soils. *In Proceedings Symposium on Evaluation of Relative Density*. Los Angeles, US. 1973. ASTM STP 523, 304-318.
121. Moser, A.P. *Buried Pipe Design, 2nd Edition*, McGraw-Hill. 2001.
122. Whitlow, R. *Basic Soil Mechanics*, 4th ed., Pearson Education Ltd. Edinburgh, England. 2001.
123. BS 1377-1. *British Standards, Methods of Test for Soils for Civil Engineering Purpose*, British Standards Institution, London. 2016.
124. Majid. Z.A., Mohsin. R. and Yusof. M.Z. Experimental and Computational Failure Analysis of Natural Gas Pipe. *Engineering Failure Analysis*, 2012. 19: 32-42.
125. McLean, A.C. and Gribble, C.D. *Geology for Civil Engineers*, 2nd edn., CRS Press, Taylor & Francis, UK. 1985.
126. Feda, J. *Mechanics of Particulate Materials, The Principles, Developments in Geotechnical Engineering*. Vol. 30, Czechoslovak Academy of Science, Prague. 1982.

127. Whitlow, R. *Basic Soil Mechanics*, 4th ed., Pearson Education Ltd. Edinburgh, England. 2001.
128. Meng. H.C. and Ludema. K.C. Wear Models and Predictive Equations: their form and Content. *Wear*, 1995. 181-183: 443-457.
129. Parsi. M., Najmi. K., Najafifard. F., Hassani. S., McLaury. B., and Shirazi. S.A. A Comprehensive Review of Solid Particle Erosion Modelling for Oil and Gas Well and Pipelines Application. *Journal of Natural Gas Science and Engineering*, 2014. 21: 850-873.
130. Ahlert. R.A. *Effect of Particle Impingement Angle and Surface Wetting on Solid Particle Erosion of AISI 1018 Steel*. Msc. Thesis. University of Tulsa; 1994.
131. Edward. J.K., McLaury. B.S. and Shirazi. S.A. Modelling Solid Particle Erosion in Elbows and Plugged Tess. *Journal of Energy Resources Technology, ASME 123*. 2001: 277-284.
132. Ghannavelu. A., Kapur. N., Neville. A., Flores. J.F. Ghorbani. N. A Numerical Investigation of a Geometry Independent Integrated Method to Predict Erosion Rates in Slurry Erosion. *Wear*, 2011. 271: 712-719.
133. Haugen. K., Kvernfold. O., Ronald. A., Sandberg. R. Sand Erosion of Wear-Resistant Materials: Erosion in Choke Valves. *Wear*, 1995. 186-187(Part 1): 179-188.
134. Neilson. I. and Gilchrist. A. Erosion by Stream of Solid Particle. *Wear*, 1968. 11(2): 111-122.
135. Forder. A., Thew. M., Harison. D. A Numerical Investigation of Solid Particle Erosion Experienced Within Oilfield Control Valve. *Wear*, 1998. 216(2): 184-193.
136. Huang. C., Chinnovelli. S., Monev. P., Nandakumar. K. Comprehensive Phenomenological Model for Erosion of Material in Jet Flow. *Powder Technology*, 2008. 187(3): 273-279.
137. Huang, C., Chinnovelli, S., Monev, P., Nandakumar, K. Comprehensive Phenomenological Model for Erosion of Material in Jet Flow. *Powder Technology. Wear*, 2010. 269: 190-196.
138. Wang. M.H., Huang. C., Nandakumar, K., Minev, P. Luo. J., Chinovelli. S. Computational Fluid Dynamics Modelling and Experimental Study of Erosion in Slurry Jet Flows. *International Journal of Computational Fluid Dynamics*, 2009. 23: 155-172.

139. Lee. B.E., Tu. J.Y., Fletcher. C.A.J. On Numerical Modelling of Particle-Wall Impaction in Relation to Erosion Prediction: Eulerian Versus Lagrangian Method. *Wear*, 2002. 252: 179-188.
140. Debhi. A. A CFD Model for Particle Dispersion in Turbulence Boundary Layer Flows. *Nuclear Engineering and Design*, 2008. 238: 707-715.
141. Gosman. A.D. and Ionnides. I.E. Aspects of Computer Simulation of Liquid Fuelled Combustors. *Journal of Energy*, 1983. 7: 482-490.
142. Tilly. G.P. Erosion Caused by Impact of Solid Particles. *Academic Press, Inc, Treatise on Material Science and Technology*, 1979. 13: 287-319.
143. Adler, W.F. Assessment of the State of Knowledge Pertaining to Solid Erosion, Final Report for Army Research Office Contract No. 1979. DAAG29-77-C-0039.
144. Nøkleberg. L. and Søntvedt. T. Erosion of Oil & Gas Industry Choke Valves Using Computational Fluid Dynamics and Experiment. *International Journal of Heat and Fluid Flow*, 1998. 19(6): 636-643
145. Anthony, K. and Nestic, S. Particle Tracking and Erosion Prediction in Three-Dimensional Bends. *Paper presented at the Proc. of ASME FED Summer Meeting*, 2000.
146. Ansys. *Fluent 15.0 Solver Theory Release 15*, Ansys Inc. 2013.
147. Vesilind. P.A. The Rosin-Rammler Particle Size Distribution. *Resource Recovery and Conservation*, 1980. 5: 275-277.
148. Nguyen. Q. B., Nguyen. Q.B., Liu. Z.G., Lim. C.H.Y, Zhang. Y.W. A Combined Numerical-Experimental Study on the Water-Sand Multiphase Flow Characteristics and The Material Erosion Behavior. *Wear*, 2014. 319: 96-109.
149. Mansouri. A., Arabnejad. H., Shirazi. S.A., McLaury. B.S. A Combined CFD/Experimental Methodology for Erosion Prediction. *Wear*, 2015. 332-333: 1090-1097.
150. Gandhi. M.B., Vuthaluru. R., Vuthaluru. H., French. D., Shah. K. CFD Based Prediction of Erosion Rate in Large Scale Wall-Fired Boiler. *Applied Thermal Engineering*, 2012. 42: 90-100.
151. Song. X.J., Park. J.H., Kim. S.G., Park. Y.C. Performance Comparison and Erosion Prediction of Jet Pumps by Using Numerical Method. *Mathematical Computer Modelling*, 2013. 57: 245-253.
152. Darihaki. F., Hajidavalloo. E., Ghasemzadeh. A., Abbas Safian. G. Erosion Prediction for Slurry Flow in Choke Geometry. *Wear*, 2017. 372-373: 42-53.

153. Chen. J., Wang. Y., Li. X., He. R., Han. S., Chen. Y. Erosion Prediction of Liquid-Particle Two-Phase Flow in Pipeline Elbows Via CFD-DEM Coupling Method. *Powder Technology*, 2015. 275: 182-187.
154. Mansouri. A., Arabnejad. H., Karimi. S., Shirazi. S.A., McLaury. S. Improved CFD Modelling and Validation of Erosion Damage Due to Fine Sand Particle. *Wear*, 2015. 338-339: 339-350.
155. Xu. L., Zhang. Q., Zheng. J., Zhao. Y. Numerical Prediction of Erosion in Elbow on CFD-DEM Simulation. *Powder Technology*, 2016. 302: 236-246.
156. Wang. K., Xiufang. L., Wang. Y., Renyang. H. Numerical Investigation of The Erosion Behavior in Elbows of Petroleum Pipelines, *Powder Technology*, 2017. 214: 490-499.
157. Habib. M.A., Badr. H.M., Ben-Mansour. R., Kabir. M.E. Erosion Rate Correlations of a Pipe Protruded in An Abrupt Pipe Contraction. *International Journal of Impact Engineering*, 2007. 34 (8): 1350-1369.
158. Habib. M.A., Ben-Mansour. R., Badr. H.M., Kabir. M.E. Erosion and Penetration Rates of a Pipe Protruded in A Sudden Contraction. *Computational Fluids*, 2008. 37 (2): 146-160.
159. Najafifard. F. *Predicting Near Wall Particle Behavior with Application to Erosion Simulation*, PhD. Thesis. University of Tulsa; 2014.
160. DeCorso, S. M. and Kothmann, R.E. Erosion by Liquid Impact. *Symposium on Erosion and Cavitation*. 1961. 3: 32-45.
161. Brunton, J. H. 1961. Deformation of Solid by Impact of Liquids at High Speeds. *Symposium on Erosion and Cavitation*. 1961. 6: 83-98.
162. Leith, W. C. and Mslquham, W.S. Accelerated Cavitation Erosion and Sand Erosion. *Symposium on Erosion and Cavitation*. 1961. 4: 46-69.
163. Reynold, K. W. and Loren, R. A. *Structural Mechanics of Buried Pipe*, CRC Press. 2000.
164. *Earth Manual, Unites States Bureau of Reclamation*, Part 1, Third Edition, 1998: 255-260.
165. *Earth Manual, Unites States Bureau of Reclamation*, Part 2, Third Edition, 1990, USBR 5515.
166. ASTM D 698-12. *Standard test methods for laboratory compaction characteristics of soil using standard effort (12 400 ft-lbf/ft³ (600 kN-m/m³))*. ASTM International, US. 2014.

167. Humprey. J. Fundamentals of Fluid Motion in Erosion by Solid Particle Impact. *International Journal of Heat and Fluid Flow*, 1990. 11: 170-195.
168. Syamlal, M. and O'Brien, T. Computer Simulations of Bubbles in a Fluidized Bed. *AIChE Symposium Series*. 1989. 85: 22-31.
169. Lun. C.K.K., Savage. S.B., Jeffrey. D.J., Chepuruiy. N. Kinetic Theories for Granular Flow: Inelastic Particles in Coquette Flow and Slightly Inelastic Particles in a General Flow Field. *Journal Fluid Mechanics*, 1984. 140: 223-256.
170. Gidaspow. D., Seo. Y., Ettehadieh. B. Hydrodynamics of Fluidization: Experiments and Theoretical Bubble Sizes in A Two-Dimensional Bed with a Jet. *Chemical Engineering Communication*, 1983. 22: 253-272.
171. Karimi. A., Schmid, R.K. Ripple Formation in Solid-Liquid Erosion. *Wear*, 1992. 156: 33-47.
172. Desale. R., Bhupendra. K., Gandhi. K., Jain. S.C. Particle Size Effects on The Slurry Erosion of Aluminium. *Wear*, 2009. 266: 1066-1071.
173. Levy. A.V. and Chik. P. The Effect of Erodent Composition and Shape on the Erosion of Steel. *Wear*, 1983. 89: 151-162.
174. Arabnejad. H., Shirazi. S.A., Mc Laury. B.S., Subrani. H.J., Rhyne. L.D. The Effect of Erodent Particle Size Hardness on The Erosion. *Wear*, 2015. 332-333: 1098-1103.
175. ASTM D1557-12. *Standard Test for Laboratory Compaction Characteristics of Soil Using Modified Effort*. ASTM International, US, 2012.
176. Viegas. D.X. and Borges. R.J. An Erosion Technique for the Measurement of the Shear Stress Field on a Flat Plate. *Journal of Physics: Sci Instrumentation*, 1986. 19: 625-630.
177. Liu. Z.G., Wan. S., Nguyen. V.Q., Zhang. Y.W. A Numerical Study of the Effect of Particie Shape on the Erosion of Ductile Materials. *Wear*, 2014. 313: 135-142.
178. Manzar. M.A. and Shah. S.N. Particle Distribution and Erosion During the Flow of Newtonian and Non-Newtonian Slurries in Straight and Coiled Pipes. *Engineering Applications of Computational Fluid Mechanics*, 2009. 3: 296-320.
179. Nguyen. V. B., Nguyen. Q.B., Zhang. Y.W., Lim. C.H.Y, Khoo. B.C. Effect of Particle Size on Erosion Characteristics. *Wear*, 2016. 348-349: 126-137.
180. Nguyen. Q. B., Lim. C.H.Y Nguyen. V.B., Wan. Y.M., Nai. B., Zhang. Y.W., Gupta. M. Slurry Erosion Characteristics and Erosion Mechanisms. *Wear*, 2014. 79: 1-7.